General Electric Research

PR Subramanian (PI)
Min Zou
Vandana Rallabandi
Joseph Zierer
Shenyan Huang

Oak Ridge National Laboratory

Orlando Rios (PI)
Hunter Henderson
Craig Bridges
Michael Brady

Dual Phase Soft Magnetic Laminates for Low-cost, Non/Reduced-Rare-Earth Containing Electrical Machines

June 30, 2020
FINAL PUBLISHABLE REPORT

This material is based on work supported by the Department of Energy under Award DE-E0007755.

GE Research – FINAL TECHNICAL REPORT

Version # 1 / June 30, 2020

Dual Phase Soft Magnetic Laminates for Low-cost, Non/Reduced-Rare-Earth Containing Electrical Machines

Primary Recipient: GE Research, PR Subramanian
Partner: Oak Ridge National Laboratory
Carpenter Technology Corp.
Applinetics Engineering LLC.

Project Start Date: 10/01/2016
Project End Date: 3/31/2020

Classification

This report is:

Draft	
Final	✓
Internal	
Public	

Recipient Address and Contact Information

PR Subramanian
GE Research
One Research Circle
Niskayuna, NY 12309
Phone: (518) 387-6154
Fax: (518) 387-6232
Email: subrampr@ge.com

Nathan Forbes
GE Research
One Research Circle
Niskayuna, NY 12309
Phone: (518) 387-6906
Fax: (518) 387-5449
Email: forbes@ge.com

General Electric Research Team

Motor Development:

James Graham
Di Pan
Robert Pietrocola
Vandana Rallabandi
Yichao Zhang
Joseph Zierer

(previous GER employees)
Karthik Bodla
Anoop Jassal
Patel Reddy

Materials Development:

Steve Buresh
Sue Corah
Shenyan Huang
Christopher Klapper
Lawrence Kool
PR Subramanian
Changjie Sun
Yongxiang Wang
Wanming Zhang
Min Zou

(previous GER employees)
Peter Bonitatibus
Francis Johnson
Tong Hui

Executive Summary

To accelerate the mass market adoption of electric drive vehicles, the key technology barriers in electric motors are (1) magnet cost and rare-earth element price volatility; (2) non-rare-earth electric motor performance; and (3) materials property optimization.

The goal of this project was to address these barriers by advancing a unique and innovative dual phase soft magnetic material technology and demonstrating the material in a 30-kW synchronous reluctance motor without using any permanent magnet for electric vehicles. Dual phase magnetic materials offer the electric motor designer the ability to locally control the magnetic saturation level in a motor laminate, while at the same time enhancing the mechanical strength of the laminate material, resulting in an enhancement in motor performance and efficiency.

Scalable dual phase soft magnetic laminates manufacturing technologies were developed in collaboration with multiple US manufacturers. 1000 lbs of alloy sheet with a thickness of 0.25mm and width of 280 mm was manufactured within the specifications. Batch sizes of up to 240 laminates per run were produced from the alloy sheet.

Two prototype motors with dual phase soft magnetic laminates were designed, built, and tested. The major goal of building the subscale prototype as a pathway to develop scalable manufacturing technologies for the dual phase soft magnetic laminates was met. The additional goal of building and testing the subscale prototype in order to validate the calculated performance with the tested motor performance was also met.

For the full-scale 30kW continuous power synchronous reluctance motor prototype, the tested performance met the targets in terms of continuous power at the operating speeds up to 8000 rpm. Post-test studies were conducted and the root causes for the discrepancy between the predicted and tested peak power, continuous power at high speed range, and efficiency were identified. Further modeling study showed that the dual phase rotor machine has a 27% higher torque to active weight ratio than an equivalent performance silicon steel rotor machine.

Application space and multiple discussions with traction motor and electric vehicle manufacturers for commercialization of the dual phase soft magnetic material technology were identified and conducted. An initial cost model was established based on the developed manufacturing technologies with the US manufacturers. Future paths for further cost reduction were identified, including increasing the market volume by broadening the applications of the dual phase soft magnetic laminate technology for electric machines in other energy sections such as oil & gas, heating, ventilation, and air conditioning (HVAC), and power generation.

Project Objectives

Project Goal

The project goal was to demonstrate scaled-up manufacturing of the dual phase magnetic materials and demonstrate a full-scale traction motor to achieve the performance targets shown in Table 1 without using any permanent magnets:

Table 1. Full-scale motor prototype performance targets based on the FREEDOMCAR 2020 advanced traction motor requirements

Parameter	Target
Peak Power (kW)	≥55
Continuous Power (kW)	≥30
Specific Power (kW/kg)	≥1.6
Power Density (kW/l)	≥5.7
Maximum Speed (rpm)	14,000
Maximum Efficiency (%)	≥96
Cost ($/kW)	≤4.7

Another goal was to establish a US supply chain by partnering with a primary metal producer for alloy production and an electric vehicle motor manufacturer for prototype motor fabrication. ORNL was responsible for measuring data on the fundamental material properties needed to optimize dual phase material processing. The market transformation plan was to be developed using input from all the partners, including market analysis and product development plans.

Approach

Two motor prototypes were fabricated using the dual phase material: 1) A subscale prototype with a continuous power rating of ≈3.7 kW was fabricated in the second year of the effort to demonstrate dual phase alloy process improvement; 2) a full-scale prototype with a continuous power rating of ≈30 kW was fabricated in the third year of the effort to demonstrate a manufacturable machine that can be tested in an operational environment.

Accomplishments

- Produced 1,000 lbs of custom dual phase alloy sheet; the measured material properties met or exceeded the magnetic, mechanical, chemistry, and dimensional requirements.
- Improved manufacturing process and achieved better control of material properties in terms of magnetization and core loss.
- Established a US supplier chain for scalable dual phase rotor manufacturing.
- Demonstrated >20% performance improvement by the dual phase material in the subscale motor by calculation.
- Built and tested the subscale motor prototype, demonstrated that the tested performance matches calculated performance.
- Designed, built and tested the 30kW full-scale motor prototype, and demonstrated a manufacturable machine that can be tested in an operational environment.

Scientific and Technical Results

Task 1.0: Produce detailed machine designs

Synchronous reluctance type motor was chosen to achieve the performance targets without using any permanent magnets. This addressed the barriers to reach the DOE VTO Electric Traction Drive System technical targets in the aspects of magnet cost, rare-earth element price volatility, and non-rare-earth electric motor performance. The dual phase material was only used in rotor laminations where the high tensile strength of the non-magnetic region (2x that of the magnetic regions) was most beneficial. Additionally, rotor laminations are typically less magnetically saturated compared to stator laminations, making them the appropriate choice for the dual phase materials' magnetic saturation level target of 1.50 ± 0.1 Tesla.

1.1 Subscale prototype design

A synchronous reluctance motor's rotor was designed with the dual phase laminates, which was retrofitted to an off-the-shelf 3.7 kW induction motor stator. The main purpose for designing, building, and testing the subscale prototype was to validate the performance prediction from calculation and to develop the scalable dual phase rotor laminates manufacturability, to save the time, labor, and materials cost for designing and building the stator of a full-scale motor.

The designs of interest considered for the prototype are (a) Four-layer, (b) Two-layer, and (c) One-layer designs as shown in Figure 1. The calculated motor performance shown in Figure 2 indicate that the 4-layer design outperforms in terms of the saliency, power, and power factor. Although the performance of the 2-layer design is very close to that of the 4-layer, the 4-layer design was selected for the subscale prototype. The reason is that the number of non-magnetic regions in the 4-layer design is 70% more than that in the 2-layer design. The sizes of the non-magnetic regions are also smaller than those of the 2-layer design. These features impose more challenges for the dual phase laminate manufacturing. Since one of the main purposes for designing and building the subscale prototype was to retire the dual phase laminates manufacturing risks, the 4-layer design was selected in order to obtain more opportunities to tackle more potential challenges.

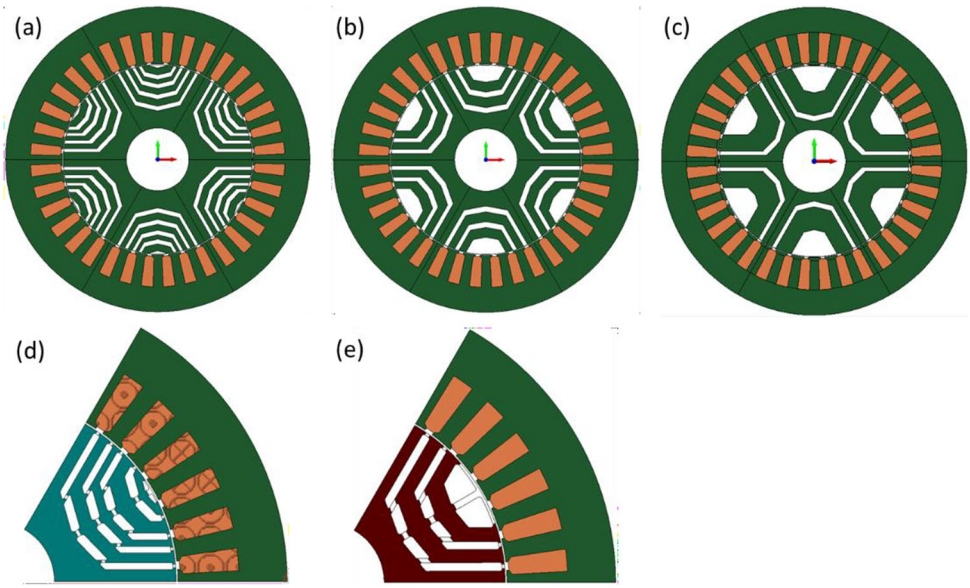

Figure 1. The cross sections of the (a) four-layer, (b) two-layer, and (c) one-layer designs with dual phase rotors. (d) (e): the detailed views of one pole of the four-layer and two-layer designs, respectively.

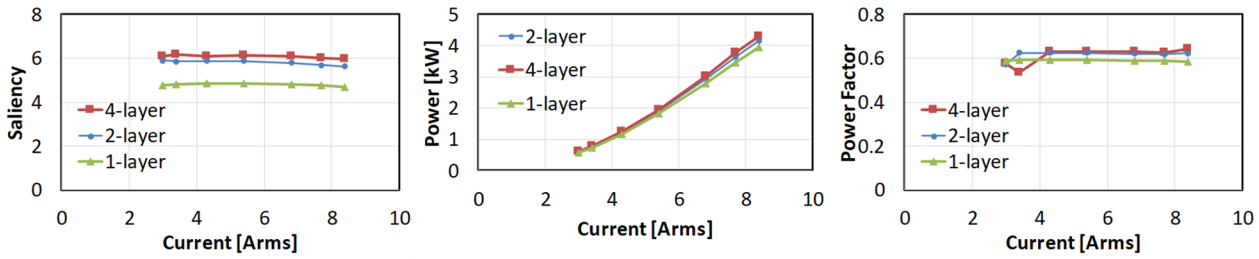

Figure 2. Subscale dual phase motor performance of the four, two, and one-layer designs

The subscale prototype design work also studied tradeoffs between the motor performance and dual phase laminates' magnetic properties in the following four aspects. The results provided the foundation for determining the priorities in the dual phase laminates manufacturing process control.

(1) The effect of magnetic permeability

Two sets of data with different magnetic properties were used in the subscale prototype design model. The data were collected on ring cores subjected to different processing conditions. For this analysis, the posts and bridges were treated as air, i.e., an ideal condition for the properties in these regions, to focus on the effect of the magnetic phase property. Figure 5 shows the dc magnetization (BH) curves and the torques generated by using these two sets of data, keeping all other design parameters the same. As expected, the material with the higher permeability leads to a higher torque.

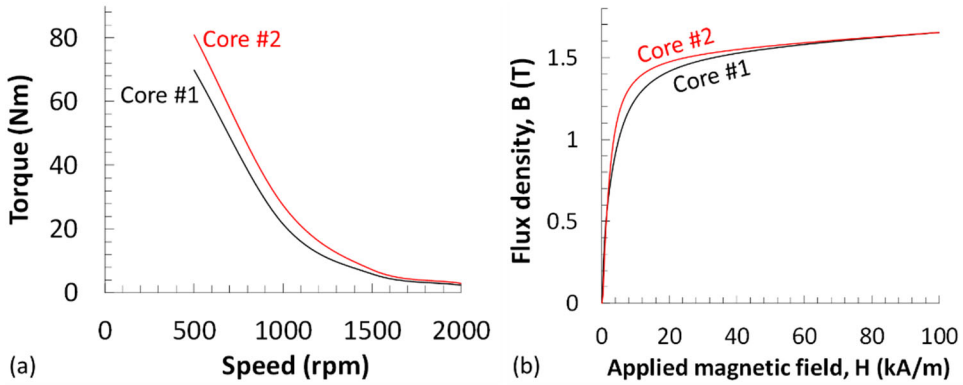

Figure 5. (a) Comparison of the torque output of the subscale motor prototypes made of (a) the dual phase rotor material with different magnetic properties.

(2) The effect of residual magnetization in the non-magnetic regions

Residual magnetization is likely to exist in the non-magnetic regions due to the processing control variation during the manufacturing. This is suspected to allow for flux leakage in these regions thus degrading motor performance. Hypothetical data of saturation magnetization between 0.01 to 0.5 T were generated in the non-magnetic regions and fed into the design model. The property data in the magnetic regions were taken as those of Core #1 as shown in Figure 5 (b). The calculated results shown in Figure 6 (a) indicate that the residual magnetization from 0.01 T to 0.5 T in the non-magnetic regions has negligible effect on torque output.

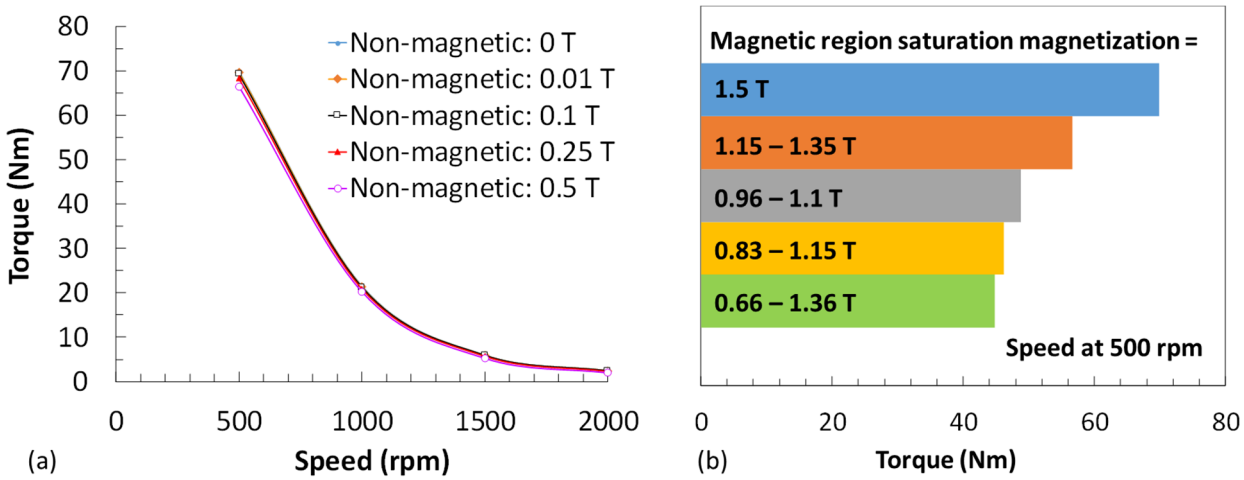

Figure 6. (a) Torque vs. speed with varying non-magnetic region saturation magnetizations; (b) Torque generated at 500 rpm with varying magnetic region saturation magnetizations, calculated based on the subscale motor prototype design.

(3) The effect of lower saturation magnetization in the magnetic regions

The material manufacturing process control variation also may lead to lower saturation magnetization in the magnetic regions. The effect of this variation has also been studied and the results are shown in Figure 6 (b). In contrast to the variation in non-magnetic region saturation magnetization, the variation in the magnetic regions has significant impact on the torque output. The results shown in Figure 6 provide valuable information for processing control in the dual phase laminates manufacturing, i.e. a more stringent control on the magnetic regions than on the non-magnetic regions has more significant impact on the motor performance.

(4) The effect of variation of the saturation magnetization

The saturation magnetizations of randomly selected subscale motor prototype laminates were measured with 100 specimens. The average magnetizations in the magnetic and non-magnetic regions were 1.50±0.03T and 0.043±0.042T, respectively. To evaluate the effect of these variations of the saturation magnetization on motor performance, the dual phase rotor was divided into multiple regions, as shown in Figure 7(b). Each region was assigned to a certain B-H curve generated by using a random distribution function with the measured mean and standard deviation values. The calculated torque vs. speed result [Figure 7(c)] shows that these small variations lead to a 10% to 15% decrease of the torque compared with the ideal case of a uniform B-H curve over the whole rotor volume [Figure 7(a)].

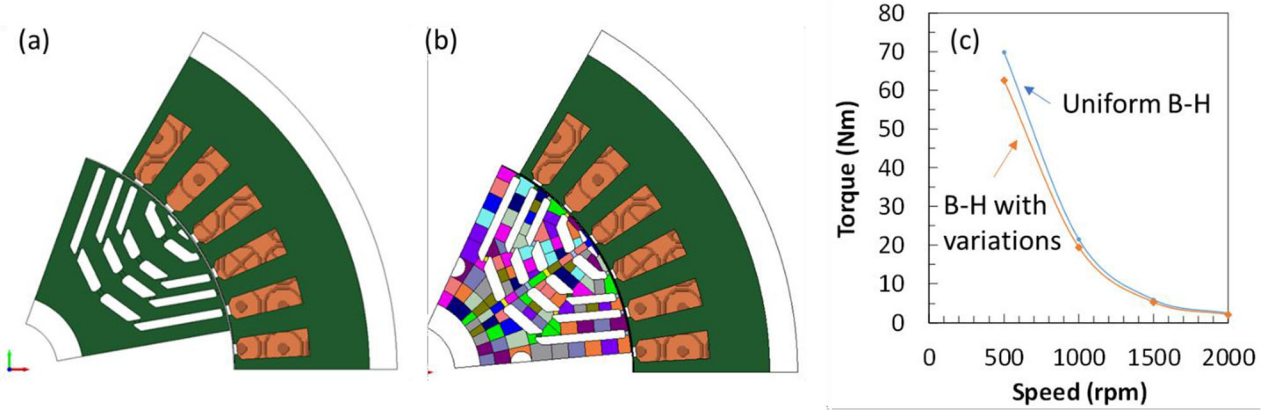

Figure 7. (a) Model with uniform B-H curve; (b) Model with varied B-H curves; (c) Comparison of the torques from the models shown in (a) and (b).

1.2 Full-scale prototype design

1.2.1 Electromagnetic design

Basic sizing study has been conducted under the DOE Award DE-EE0005573. The active mass of machine and saliency under peak and maximum speed operations have been calculated with 6, 8, 10, and 12 poles and 1, 2, 3, 4, and 5 layers. The results show that a 2-layer and 6- or 8-pole design is sufficient to meet the machine performance targets.

The reported project design team conducted a more detailed analysis based on the prior study. A comparison of the motor performance between the 6- and 8-pole designs (Table 2) shows that the 8-pole design provides a higher efficiency and lighter weight than the 6-pole design. After choosing the 8-pole design, a comparison between the 2- and 3-layer designs (Table 3) indicate that the 2-layer design has slightly better performance. Therefore, the 2-layer 8-pole design was chosen for the full-scale motor prototype, also taking the trade-off between the machine performance and manufacturing cost into consideration. Fewer layers and poles have the advantage of less manufacturing complexity, thus costing less.

The final design parameters and calculated machine performance are listed in Table 4. The calculated performance met the project targets in terms of continuous and peak power, power density, and specific power. The specific power was calculated based on active materials' mass including rotor and stator cores and windings, excluding the rotor shaft. The flux density maps of this design shown in Figure 8 illustrate the absence of flux leakage as commonly seen in the conventional silicon steel rotors.

1.2.2 Mechanical design

1.2.2.1 Subscale Motor Design

The subscale test motor was built by retrofitting the dual phase rotor into a commercial induction motor with a rated power of 3.7 kW. For adaption to the subscale motor testing, critical rotor components were disassembled and accurately measured. The measured data were used to develop a SolidWorks model, which was used to create the drawings for new components, make modifications to existing components, and develop assembly tooling. In addition, the models were used to develop assembly procedures. These procedures have been used to drive the tooling requirements and allowed the team to discuss and develop a low risk assembly approach.

1.2.2.2 Full Scale Rotor Stress Analysis

The stress analysis of the full-scale rotor under the expected assembly and operating speeds was conducted using a finite element analysis (FEA) software, ANSYS. The results are shown in Figure 9. The fit between the laminated rotor core and the shaft was accomplished with an interference fit, allowing the effective transfer of torque and serving as a pathway for additional heat transfer. As such, this interface was carefully evaluated to make sure there is adequate interference pressure, but not too much to impose excessive stress into the laminated rotor structure. Based on the analyses, the radial interference between the rotor shaft and lamination needs to be 0.002-0.003 inch, which is typical for rotor assemblies in this size and speed range and allows for some manufacturing tolerances. Additionally, the equivalent (Von Mises) stresses reach a maximum value of {} in the bridges and post regions of the rotor laminations, depending on the speed and selected interference. Further analysis shows that the maximum speed that this dual phase rotor design can achieve is {}, with a {} radial interference, based on the balance between the assembly induced stress and transferring torque at the full speed.

1.2.2.3 Full Scale Rotor Dynamics Analysis

The rotor dynamics analysis results shown in Figure 10 predict that the first critical speed is well above the operating speed.

1.2.2.4 Full Scale Motor Design

A conceptual design for full scale 30 kW continuous duty motor was completed first, followed by incorporating additional details. The conceptual design provided manufacturing partners a clear vision of what features and characteristics are needed in the full-scale prototype. This design was based on several successful prototypes that have been previously manufactured and tested at GE Research. The initial layout helped manufacturing partners provide a better estimate of the time and materials needed to fabricate and test the full-scale prototype. It was also used internally to help identify the best suitable dynamometer, torque transducer selection, power electronics, and laboratory- based cooling system.

The further detailed design work involved design and calculation of interface fits under different operating conditions, creation of bill of materials, and development of the electrical terminal box.

1.2.3 Thermal design

The thermal management strategy for the dual phase prototype motor utilizes two methods of cooling in the armature, a combination of indirect and direct cooling.

The second method, a direct cooling approach, includes spraying coolant (oil, for example) directly onto the end turns to remove excess heat very effectively. However, steps need to be taken to prevent the coolant from migrating into the space between the rotor and stator, the air gap. Allowing too much coolant into the air gap could generate a significant amount of frictional heating and would counteract the desirable cooling achieved through end turn spraying. Additionally, the end turn coolant will collect in the bottom of the motor housing and needs to be removed with a scavenging system.

Task 2.0: Develop materials

2.1 Produce rolled alloy sheet

A 1000-lb coil of alloy sheet was produced by Carpenter Technology Corporation. The alloy composition, magnetic properties, mechanical properties, and dimensions of the sheet were all within specification. Figure 15 shows a sample piece cut from the coil and one of the coils as received.

[3]

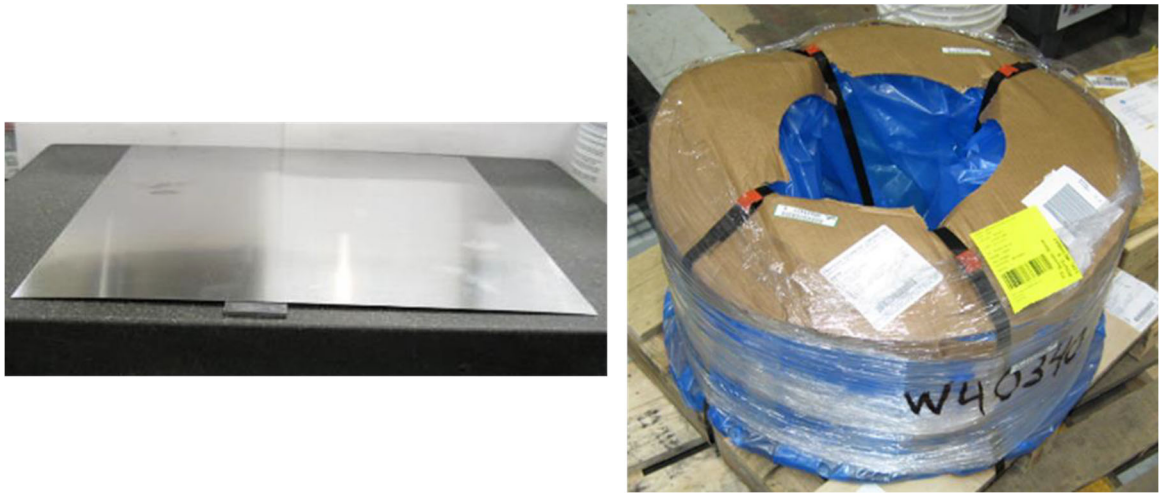

Figure 15. Rolled alloy sheet sample piece (left) and coil (right).

In a prior project (DE-EE0005573), a subscale dual phase rotor was manufactured using GE Research lab-scale facilities. Extensive effort has been devoted to the reported project to develop scalable processes with various industrial partners. The processing practices and scalability assessments are described below following the fabricating sequence as outlined in Figure 16.

3.1.1. Cut the rotor laminates

For the 525 pieces of subscale prototype rotor laminates, although the cutting was carried out by laser due to the insufficient volume for stamping, no risk is foreseen to use the conventional high-volume low- cost stamping technology to make the laminates, given the thickness (0.25mm) and ultimate tensile strength (655 MPa) of this material in its as-cold-rolled state.

3.1.2. Coat with ceramic mask

Ceramic mask slurry was coated on both sides of the laminates using a spray gun with controlled speed, pressure, and time duration. The correlation between the spray gun setting parameters and the coating thickness was established by design of experiments. The spraying coating process parameters were proved to be well controlled to provide sufficient protection from the nitrogen penetration during the subsequent nitrogenating heat treatment.

The coatings on the bridges and posts of the laminates were then removed by grit blasting while keeping the other regions masked by tooling templates. The grit blasting media size, pressure, and time duration were also optimized based on experimental results.

The spraying coating and grit blasting are mature technologies. The developed coating process parameters can be easily transferred to scale-up process and integrated with process automation to achieve high-volume and low-cost.

2.2.3 Nitrogenate laminates

Multiple types of heat treatment fixture materials and designs were experimented to provide support while ensure sufficient nitrogen gas flow and fast cooling rate to transform the bridges and posts into the non-magnetic phase.

The heat treatment parameters including the ramping and cooling rates, temperature, time duration, and atmosphere control were established by design of experiments based on thermodynamic and kinetic calculations and prior lab-scale coupon test results. Heat treatments with a batch size of 240 laminates were successfully conducted in industrial furnaces with a hot zone size up to 36” wide, 30” high, and 50” deep, which has the capability to heat treat more than 1000 laminates per run.

2.2.4 Strip coating

After nitrogenating heat treatment, the ceramic coatings on the magnetic regions of the laminates were removed by grit blasting. The grit blasting media size, pressure, and time during were successfully controlled to avoid deformation caused by this process step. These process parameters will also be used in an automatic grit blasting line to achieve high-volume and low-cost.

2.2.5 Apply insulation, stack and bond rotor, assembly prototype

Technologies used for these three steps are the same as for conventional laminated electrical steel rotors.

The development work conducted on the masking, heat treating, and demasking of the dual phase rotor in the reported project has led to improved control of the saturation magnetization within the two phases, reduction of AC core loss, and refinement of the heat treatment cycle, as shown in Figure 17.

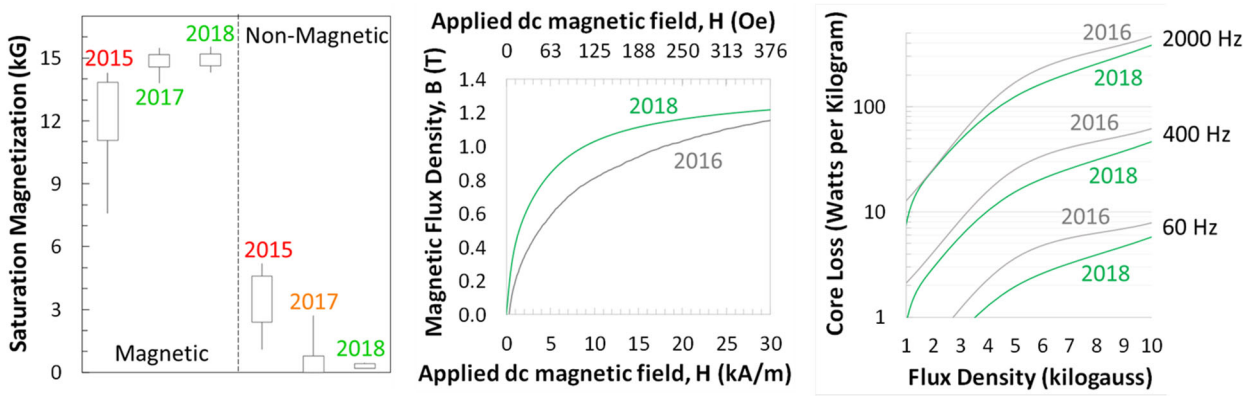

Figure 17. Improved magnetic and core loss properties by improved processing controls evolved from 2015 to 2018.

3.2 Fabricate full-scale rotor

After retiring the manufacturing risks during the process development in the subscale rotor, 275 pieces of 20 cm outer diameter dual phase laminates with a stack length of 7 cm were manufactured with the collaboration between several US engineering and heat treatment service suppliers, including Polaris Laser Laminations LLC., Solar Atmospheres Inc., and Guyson Corporation of USA. The pictures of the laminates and stacked rotor core are shown in Figure 18. The fabricated rotor demonstrated magnetic and mechanical properties within specification. Figure 19 shows a randomly selected specimen cut from a full-scale rotor laminate, and the measured saturation magnetization across this specimen. The data show excellent control of the saturation magnetization in both phases.

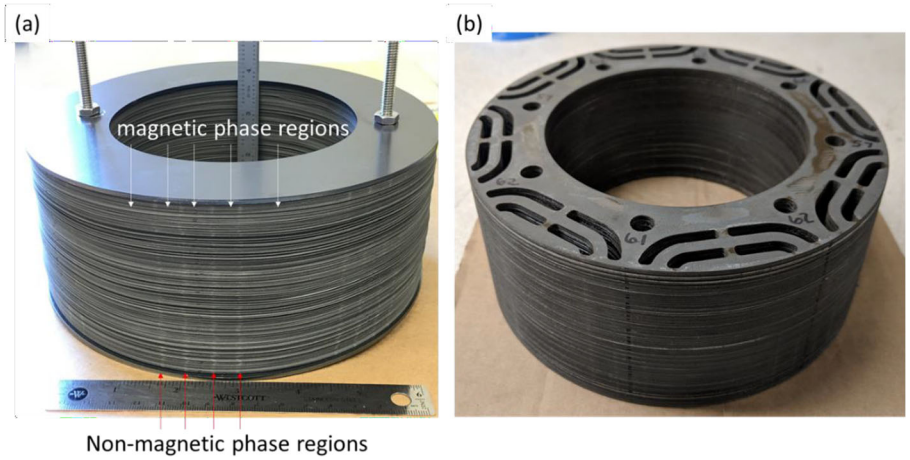

Figure 18. (a) Full-scale dual phase laminates; (b) Stacked and bonded dual phase rotor core.

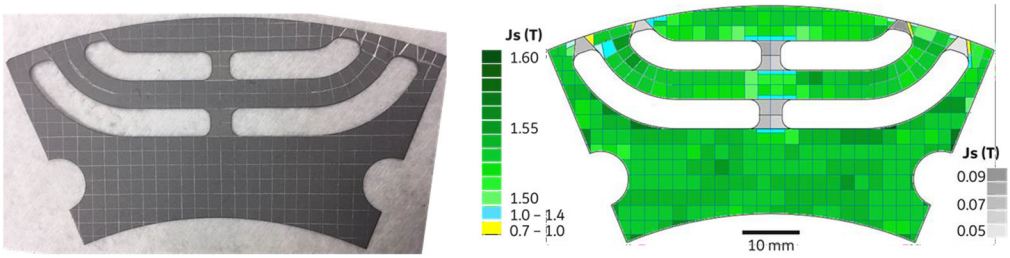

Figure 19. (a) A randomly selected specimen cut from a full-scale rotor laminate, and (b) the measured saturation magnetization across this specimen.

3.3 Evaluate nitriding kinetics and residual stress

Solution nitriding kinetics to transform the magnetic to non-magnetic phase were studied both theoretically and experimentally. The results shown in Figure 20 indicate good agreement between the calculation and measurements. For the 0.25mm thick sheet used for this project, 10 to 15 minutes exposure to a gas nitrogen atmosphere was sufficient for a complete phase transformation, which is beneficial for low cost manufacturing compared with long-term treatment cycles.

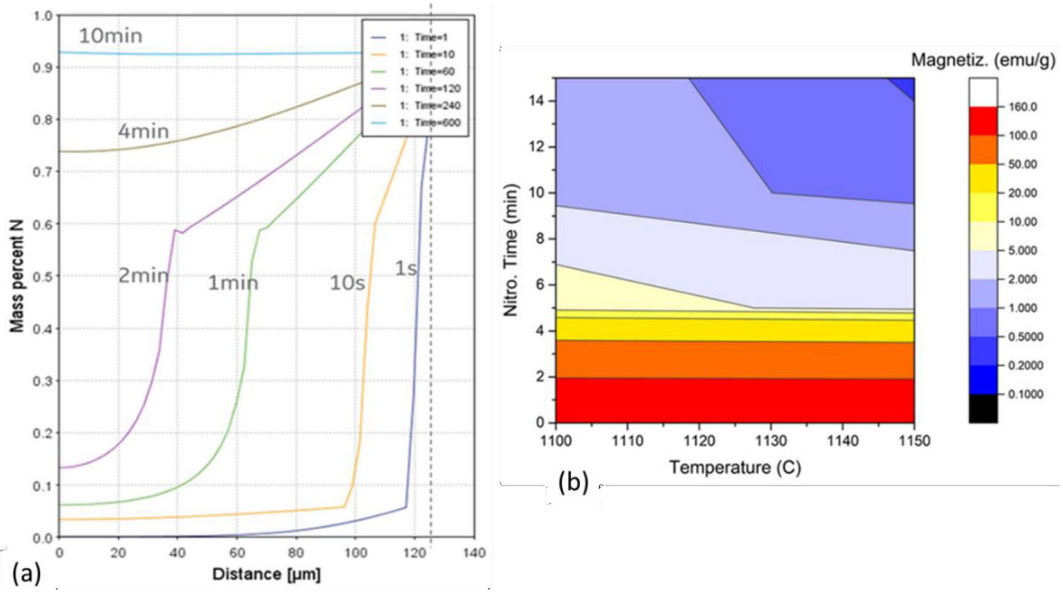

Figure 20. Solution nitriding kinetics (a) predicted based on numerical solution of the multi-component diffusion equations by using the Diffusion Module (DICTRA) in the Thermo-Calc® Software, and (b) illustrated in the experimentally established time-temperature-magnetization contour map.

The ORNL team developed the residual stress analysis method using an XRD Portable Residual Stress Measurement System. The experimental results on a nitrogenated laminate indicated that there are significant residual surface stresses in the radial direction. The data from different locations on the laminate indicate that the residual stresses after nitrogenation heat treatment may not be uniformly distributed, which agrees with the calculated stress distribution conducted by GE mechanical engineers.

In 2019, the team devised a method of probing residual strain much deeper into the rotor than would be possible with X-rays. The analysis method is shown schematically on a single rotor laminate in Fig. 21 (a). Two particular line scans of interest are discussed here, a line that included several transitions from magnetic to nonmagnetic sections and back, and another line that was entirely in magnetic areas. The static 90° angle between incident beam and detector meant that to minimize beam attenuation through the steel, the geometry in Fig. 21 (b) was used. Additionally, a voxel size of 2x2x2 mm^3 was used.

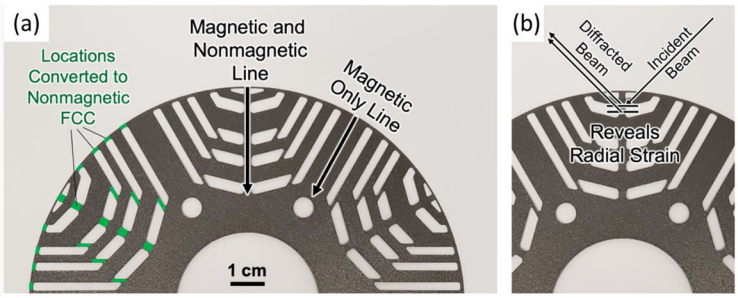

Fig. 21. Rotor laminate and analysis geometry. (a) Photograph of an individual laminate showing which locations are transformed into non-magnetic austenite and the neutron diffraction analysis lines. (b) Geometry of incident and diffracted beam, showing that the measured d-spacing and corresponding strain is radial to the laminate.

Surface plots of the diffraction spectra intensity from both line-scans as a function of distance into the rotor are shown in Fig. 22. Examples of ferromagnetic body center cubic (BCC) and austenitic non-magnetic face center cubic (FCC) phase peaks are labeled. It can be seen that there is an alternation between BCC and FCC diffraction intensity in the analysis regions, as expected. Conversely, in the magnetic only line, a steady BCC signal is seen, though attenuation of the signal is clear, as the analysis region reaches further into the rotor.

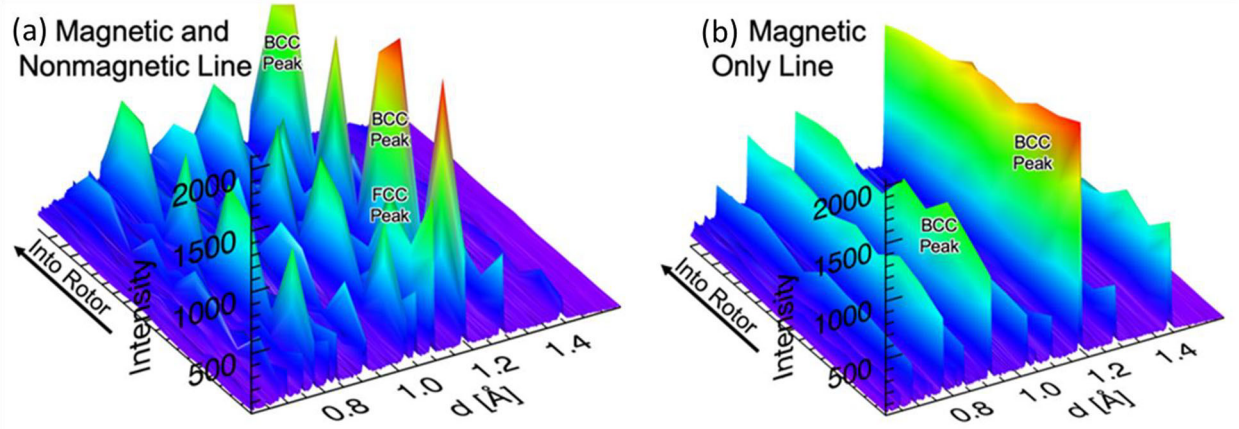

Fig. 22. Surface plots of peak intensity for (a) the magnetic and nonmagnetic lines; (b) the magnetic only line. A modulation between BCC and FCC peaks can be seen in (a) and steady BCC signal is seen in (b).

The results of the analysis are shown in Fig. 23, which correlates calculated radial stress values for each relevant phase to its respective location in the line scan. Overall, radial stress in both phases is compressive, with systematically higher stress found in FCC than in BCC.

Task 3.0: Fabricate and test prototypes

3.1 Fabricate and test subscale prototype

The subscale prototype was fabricated by replacing the rotor from an off-the-shelf 3.7 kW motor with the dual phase rotor. The as-purchased motor was disassembled, and the shaft diameter at the shaft/core interface was then measured. This diameter was used to set the rotor core inside diameter, such that appropriate interference is achieved for sub-scale motor testing. This effort also provided the opportunity to find a suitable location for the optical encoder needed during testing. The steps of fabricating the subscale prototype are shown in Figure 24. The subscale motor assembly work included the rotor subassembly using the dual phase material laminations, integration of thermocouples into the stator winding, integrating a rotor position encoder, and balancing the new rotor assembly. All aspects of the subscale motor assembly went smoothly and efficiently, and many of the approaches used were carried over to the full-scale motor assembly. Before operating the motor, a series of electrical tests were completed, including winding resistance measurements, verification of insulation properties, and a surge test. Additionally, the motor was mechanically driven up to 2000 rpm to verify the absence of undesirable vibrations in the desired operating range. All bench tests were satisfactorily completed before performance testing was started.

The subscale prototype was then tested in a speed range between 400 and 2000 rpm and at three current levels between 10 and 30 A (peak). The motor was driven by the dyno dc motor in a constant speed mode, using a set of in-house power electronics that were upgraded and installed for the test. The ac current excitation was applied to the test motor at a constant torque mode. A current angle (gamma) sweep was conducted at ±1 to 2 degrees (electrical) around the predicted gamma values to locate the maximum torque per ampere (MTPA) point at each speed. The shaft torque output was measured by a torque meter. The 3-phase input voltage, current, and temperatures were measured at each operating speed. The power output, power factor, and efficiency were then derived accordingly. Vibration data and winding temperatures were recorded during the test using a multi-channel data acquisition system. The subscale motor did not require any additional cooling hardware, due to the

short duration of the tests. All of the systems used during the subscale tests were duplicated during the full-scale tests, at higher loads and speed, along with the addition of cooling hardware installed on the test stand.

Figure 25 shows the comparison of predicted and measured performance of the sub-scale prototype motor. The data show that the prototype with a rotor manufactured from 0.010" thick dual phase alloy sheet has higher power and torque output than a similarly sized prototype with a rotor manufactured from 0.010" thick Silicon Steel (the HF10 grade). These performance gains persist over a wide speed range. At low speed, the dual phase machine is measured to have 30% greater power and torque output than a silicon steel machine, exceeding the 20% performance increase target set for this project. The predicted and measured performance agrees well with each other in the low and high-speed ranges, showing less than 10% deviation. The deviation might have originated from the difference between the material properties used for calculation and in the prototype rotor. The magnetic properties used for calculation were measured using a bonded ring laminate core. Although the ring laminate core was fabricated using the same processing procedures as used for the prototype rotor laminates, different geometry and bonding stress may cause different magnetic performance.

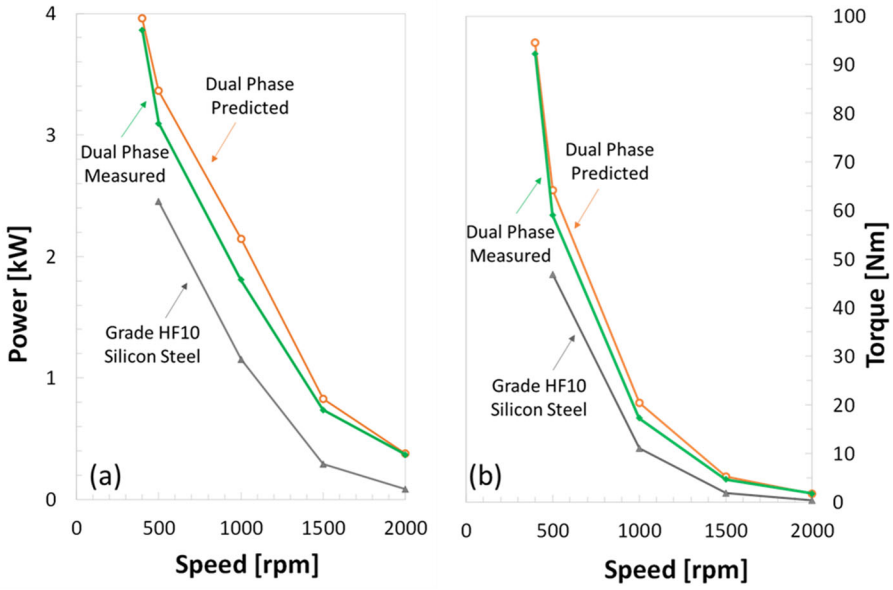

Figure 25. Measured performance of the sub-scale dual phase synchronous reluctance prototype compared with the predicted performance by design. The prototype with the rotor manufactured from the 0.010" thick dual phase sheet is measured to have at least 30% higher power and torque output than a synchronous reluctance motor with its rotor made of grade HF10 silicon steel by the same design.

3.2 Fabricate and test full-scale prototype

The full-scale prototype was fabricated by GE Research and Applinetics Engineering LLC. The motor assembly was initiated by the successful installation of the dual phase rotor core onto the rotor shaft using a shrink fit. The rotor assembly was then balanced to an ISO G1 balance, which is typical of electric motors with this size. Following the rotor assembly and balance, the armature assembly, including the assembly of the cooling sleeve onto the stator core, the stator core into the housing, and the motor endplates was carried out. The motor assembly procedure is shown in Figure 26. The exterior dimensions of the prototype motor are shown in Figure 27 (a).

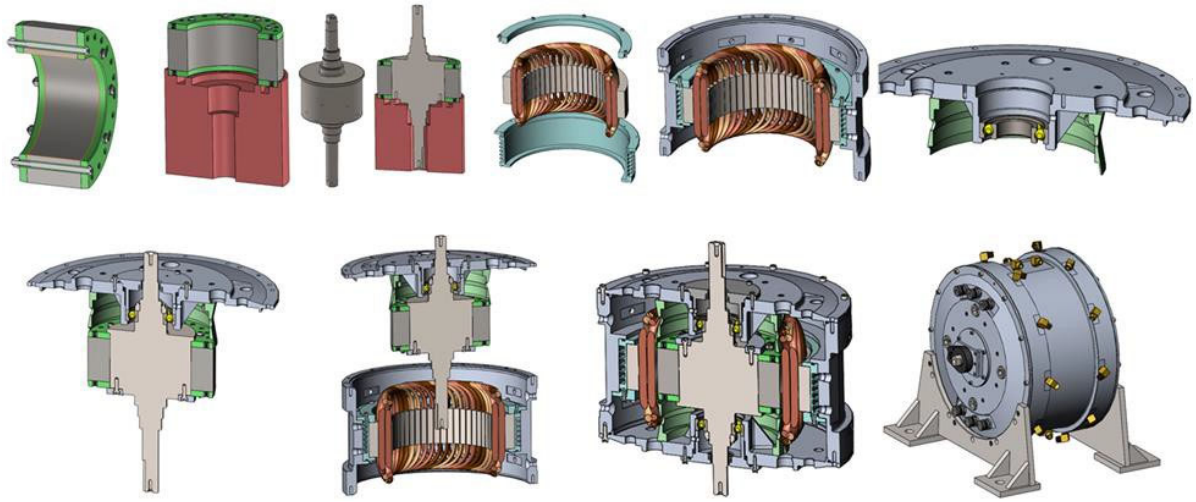

Figure 26. Motor assembly overview

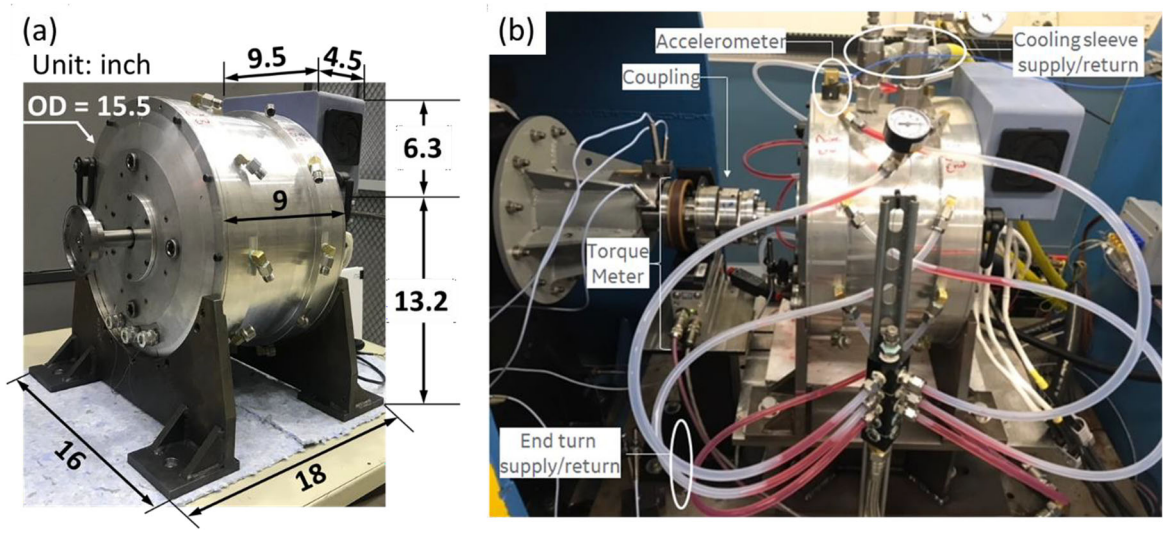

Figure 27. (a) The full-scale dual phase motor prototype; (b) the prototype on the test stand.

Meggar and Hi-pot tests up to 1000 volts were carried out and showed satisfactory insulation results. Additional capacitance and dissipation factor tests, which are non-destructive tests that provide additional insight into the insulation quality were also performed. The results show consistent capacitance and dissipation factor in all three phases, providing a higher level of confidence that the dual phase motor should be able to complete the scheduled tests.

Following the insulation tests, the full-scale motor was installed on to the dynamometer test stand. After the initial setup and alignment on the pedestal, the coupling between gearbox and dual phase motor, torque meter, and housing mounted accelerometer were also installed. Additionally, the cooling system components, including the end turn coolant (oil) supply lines, motor housing sump drain lines and pump, and cooling sleeve coolant (water/glycol) supply and return lines were attached to the motor housing, as shown in Figure 27 (b).

Prior to the performance tests, mechanical checkout runs were carried out. During these runs, test engineers checked for correct temperature measurements throughout the motor, coolant flow rates, torque measurements, and acceptable vibration levels, all of which were within acceptable levels to ensure safe operation during performance tests.

The measurements were conducted over an operating voltage range between 300 and 450 Vdc and a speed range between 500 and 12000 rpm with a maximum per-phase current of 400 A rms. A current angle (gamma) sweep was conducted at ± 1 to 2 degrees (electrical) around the predicted gamma values to locate the maximum torque per ampere (MTPA) point at each speed. The shaft torque output was measured by a torque meter. The 3-phase input voltage, current, and temperatures were measured at each operating speed. The power output, power factor, and efficiency were then derived accordingly. Heat run tests were conducted for 30 minutes at 2800, 5000, and 7000 rpm at the 30kW power output points.

The coolant flow rate, inlet pressure, coolant pressure drop, and temperature were measured at continuous power operating points.
The measured continuous power output meets the project target of 30 kW at the speed range between 2800 and 8000 rpm. The shaft torque also meets the target at speeds up to 8000 rpm. The maximum measured efficiency is 94%, which meets the FreedomCAR 2020 advanced traction motor target of 94-96%.

3.3 Post-test motor performance study

After a clear understanding of the causes for the measured and originally predicted motor performance, a new study was conducted by (i) using the rotor core material's properties measured on the specimen undergone the scalable production; (ii) using the stator core material's properties in its annealed state; (iii) using a transient instead of a static model. The study had focused on two areas:

1) Comparison of the designed synchronous reluctance motor performance with the rotors made of silicon steel grade HF10 and dual phase material;

2) Design modifications required to achieve the 55kW peak power, and 30kW high speed constant power with the rotor made of dual phase material.

3.3.1. Comparison of the designed synchronous reluctance motor performance with the rotors made of silicon steel grade HF10 and dual phase material

For the purposes of the comparison, the stators for both machines are considered to be made of HF10. In case of the synchronous reluctance machine without dual phase (DP) material, the rotor was assumed to be made of HF10 laminations. The machines are referred to as HF10Synrel and DPSynrel.

In addition to magnetic properties, the dual phase rotor material also has an advantage of higher mechanical strength in the non-magnetic phase (Table 6). The higher the material's mechanical strength, the larger the allowable rotor tip speed, which is given by

$$v = \omega r$$

where v is the rotor tip speed; ω, the angular velocity in rad/s, and r, the rotor radius.

Task 4.0: Produce market development plan

Application spaces and first products to be designed with the dual phase materials were identified in consultation with internal GE experts. Various motor designs, including synchronous reluctance and interior permanent magnet machines, with material choices were considered for balance of power density, efficiency, and manufacturing costs. Multiple efforts were initiated to identify potential partners to industrialize this class of electric machines and develop commercial markets for the dual-phase motor technology. Potential paths explored for commercialization include Tier 1 and OEM level manufacturers of motors. Potential applications include (a) small motors for electrically-driven turbochargers; (b) direct drive superchargers for heavy- duty diesel engines; and (c) traction motors.

As part of this program, an initial cost model was drafted, based on the current design of the prototype motors. The costs of electromagnetically active components were assessed from well-established cost models and engineering estimates for off-the-shelf components. Production costs of the dual-phase laminates were estimated based on well-known industrial processes for the various steps in making the dual-phase laminate material, continuous annealing/heat-treatment furnace treatments, as well as laser-etching and chemical etching systems typically used in semiconductor manufacturing processes.

The cost pareto indicated key manufacturing steps where further efforts are warranted to fully scale up the production methods. These steps include:

(1) Stamping of laminations as a replacement for current laser cutting for lamination fabrication from sheet steel, which is an industrially viable process. GE Power has extensive experience in laminate stamping for their power generator components. For a full-scale production process, industrial stamping vendors are readily available.

(2) Continuous furnaces versus batch furnaces for nitrogenation heat-treatment. Commercial belt-furnaces and continuous annealing furnaces are readily available.

(3) Masking and mask removal process for local nitrogenation: production vendors are capable of manufacturing-scale operations with process automation to lower the overall cost.

As mentioned in Task 2 of this report, the rotor fabrication suppliers are all US manufacturers. To further reduce the dual phase soft magnetic laminate costs, GE Research has initiated the licensing process to broaden potential market. The market volume of the dual phase soft magnetic material would be broadened by the applications in various electric machines in other energy sections such as oil & gas, heating, ventilation, and air conditioning (HVAC), and power generation. This initial cost model will be continually refined beyond this DOE-effort, and depending on the specific product identified for the introduction of the dual-phase laminate system, further efforts will be initiated on eventual commercialization.

Conclusion

A total of 1,000 lbs of custom dual phase alloy sheet has been produced by a US manufacturer, Carpenter Technology Corporation, with the properties meeting the specifications. Scalable manufacturing of the dual phase soft magnetic laminates has been established with multiple US suppliers. Two synchronous reluctance motor prototypes without using any permanent magnets have been fabricated and tested. The subscale 3.7 kW motor prototype demonstrated >20% performance improvement with the dual phase material rotor compared with the motor using the conventional grade HF10 silicon steel rotor. The subscale prototype demonstrated that the tested performance matches well with the calculated performance. A 30-kW continuous power motor prototype was designed, built, and tested, and demonstrated a manufacturable machine that can be tested in an operational environment.

Inventions/Patent Applications

1. Patent US10673288B2, Method for forming a nitrogenation barrier and machine formed using a body having the nitrogenation barrier, 2020-06-02
2. Patent US10501839B2, Methods of removing a ceramic coating from a substrate, 2019-12-10
3. Patent US10190206B2, Dual phase magnetic material component and method of forming, 2019-01-29
4. Patent Application US20190341821A1, Unitary structure having magnetic and non-magnetic phases, 2019-11-07
5. Patent Application US20190279795A1, Methods of making a component with variable magnetization and related components, 2019-09-12
6. Patent Application US20180337565A1, Dual magnetic phase material rings for ac electric machines, 2018-11-22